

PAPER • OPEN ACCESS

## Analysis of Electron Beam Damage of Crystalline Pharmaceutical Materials by Transmission Electron Microscopy

To cite this article: M S'ari *et al* 2015 *J. Phys.: Conf. Ser.* **644** 012038

View the [article online](#) for updates and enhancements.

You may also like

- [The effects of seaweed, \*Sargassum\* sp. meal dosages in the artificial diet on growth, feed intake, feed efficiency, protein efficiency ratio, and nutritional body composition of Rabbitfish, \*Siiganus guttatus\*](#)  
Usman, E Saade, HA Sulaeman et al.
- [Electron beam damage in oxides: a review](#)  
Nan Jiang
- [Optimal therapies of a virus replication model with pharmacological delays based on reverse transcriptase inhibitors and protease inhibitors](#)  
Yongzhen Pei, Changguo Li and Xiyin Liang



**ECS**  
The  
Electrochemical  
Society  
Advancing solid state &  
electrochemical science & technology

**DISCOVER**  
how sustainability  
intersects with  
electrochemistry & solid  
state science research

# Analysis of Electron Beam Damage of Crystalline Pharmaceutical Materials by Transmission Electron Microscopy

M S'ari <sup>1</sup>, J Cattle <sup>1</sup>, N Hondow <sup>1</sup>, H Blade <sup>2</sup>, S Cosgrove <sup>2</sup>, R M Brydson <sup>1</sup> and A P Brown <sup>1</sup>

<sup>1</sup> Institute for Materials Research, School of Chemical and Process Engineering, University of Leeds, Leeds, LS2 9JT, United Kingdom

<sup>2</sup> Pharmaceutical Development, AstraZeneca, Macclesfield, SK10 2NA, United Kingdom

E-mail: sm11msa@leeds.ac.uk

**Abstract.** We have studied the impact of transmission electron microscopy (TEM) and low dose electron diffraction on ten different crystalline pharmaceutical compounds, covering a diverse chemical space and with differing physical properties. The aim was to establish if particular chemical moieties were more susceptible to damage within the electron beam. We have measured crystalline diffraction patterns for each and indexed nine out of ten of them. Characteristic electron dosages are reported for each material, with no apparent correlation between chemical structure and stability within the electron beam. Such low dose electron diffraction protocols are suitable for the study of pharmaceutical compounds.

## 1. Introduction

The performance of pharmaceuticals is highly dependent on the structure and purity of the active pharmaceutical ingredient (API). It is essential to fully understand and characterize the solid state properties of pharmaceutical materials, different polymorphs (different crystal structures of the same compound) can exhibit different effects in the body and may require different processing and storage conditions. Characterization includes understanding what crystal forms and impurities are present within the material and in what quantity. Currently the conventional ways to determine the properties of materials are to use techniques such as powder X-ray diffraction (pXRD). These techniques are very useful for analyzing bulk materials however, current detection limits make it difficult to analyze trace amounts (<1%), materials with low crystallinity or nano-sized crystalline particles.

Transmission electron microscopy (TEM) can be applied to the characterization of pharmaceuticals, for example, through analysis of individual particles by electron diffraction, the identification of amorphous and crystalline phases present at low concentrations and identification of different polymorphs [1]. The diffraction patterns yield information on the symmetry and unit cell dimensions of the crystalline form within the material, ultimately characterizing the API and distinguish between different crystal structures. Through analysis of particles or crystals of different morphology, trace impurities can be identified and analyzed using TEM; by electron diffraction, energy dispersive X-ray (EDX) spectroscopy and potentially electron energy loss spectroscopy (EELS).

A major problem in TEM analysis of pharmaceuticals is alteration or damage due to the electron beam, especially for structurally sensitive specimens such as biological materials, polymers and



organic crystals. There are two main causes of beam damage that occur in TEM, elastic and inelastic scattering events [2, 3].

Elastic scattering occurs when electrons interact with the electrostatic field of atomic nuclei, and can result in atomic displacement or electron-beam sputtering. Inelastic scattering is caused by electron-electron interactions and can result in ionization damage (radiolysis) of the sample, this causes chemical bonds to break and change the structure of the specimen. Other forms of damage that can be caused by both elastic and inelastic scattering include electrostatic charging, hydrocarbon contamination and heating of the specimen [2, 3].

For organic compounds radiolysis is the main form of radiation damage and in some crystalline specimens this results in a decrease in crystallinity, evident in a fading electron diffraction pattern. Previous work on organic compounds has shown conjugated ring systems increase the stability of the compound in the electron beam probably due to improved intermolecular bonding [4]. Replacing hydrogen atoms with halides such as chlorine and fluorine has also been shown to improve the stability of organic compounds possibly due to an increase in steric interactions stopping other atoms from moving once chemical bonds have been broken [5].

In this study we investigated ten different crystalline pharmaceutical compounds covering a diverse chemical space and with differing physical properties to characterise and determine which chemical structures are more susceptible to electron beam damage.

## 2. Experimental

All the samples were provided by AstraZeneca after checking the crystallinity by pXRD. Samples were prepared for TEM by suspending the non-soluble powders in water and placing a drop onto an Ar/O<sub>2</sub> plasma treated, continuous carbon TEM grid and allowing it to air dry. The grids were examined by TEM (FEI Tecnai F20), operated at 200 kV and equipped with a Gatan Orius CCD camera using a standard room temperature characterization protocol established by Pan et al. [6]. Briefly, the flux of electrons was given by the irradiation time and beam intensity which was controlled by the condenser lens and electron source (extraction voltage, gun lens and spot size) settings.

The characteristic dose (electron dose when the intensity of the brightest diffraction spot falls to a value of  $1/e$ ) was obtained from a plot of normalized diffraction spot intensity versus electron fluence. The electron fluence was calculated for each diffraction pattern from the exposure time and electron beam current using a procedure described by Pan et al. [6] and the spot intensities were normalized against the most intense spot.

## 3. Results and Discussion

Diffraction pattern series were successfully gathered for ten compounds and characteristic dosages determined (Table 1). For the compounds with known structures the experimental diffraction patterns were indexed to a specific zone axis despite not lying in an exact orientation (Figure 1).

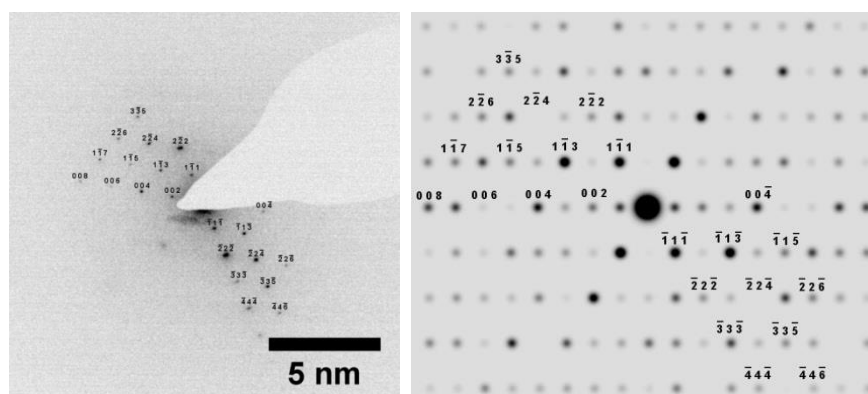


**Figure 1:** (a) Electron diffraction pattern from an indapamide crystal oriented close to the [110] zone axis, recorded with an electron flux of 3.59 electrons nm<sup>-2</sup> s<sup>-1</sup> (b) [110] pattern simulation using CrystalMaker software and indapamide structure listed in Table 1.

**Table 1:** Characteristic dosages (averages and standard deviation of three or more measurements) of specific diffraction spots for each pharmaceutical compound investigated, obtained from normalized intensity versus electron fluence plots (Figure 3).

Compound	Chemical Formula	Characteristic Dose ( $e^-$ /nm <sup>2</sup> )	Miller Indices (hkl)	CSD Refcode [7]
Tolnaftate	C <sub>19</sub> H <sub>17</sub> NOS	2079 ± 40	No available structure	No available structure
Griseofulvin	C <sub>17</sub> H <sub>17</sub> ClO <sub>6</sub>	1620 ± 160	011	GRISFL02
Indapamide	C <sub>16</sub> H <sub>16</sub> ClN <sub>3</sub> O <sub>3</sub> S	571 ± 40	$\bar{2}22$	FOCCAD
Bicalutamide	C <sub>18</sub> H <sub>14</sub> F <sub>4</sub> N <sub>2</sub> O <sub>4</sub> S	454 ± 20	002	JAYCES
Cilostazol	C <sub>20</sub> H <sub>27</sub> N <sub>5</sub> O <sub>2</sub>	297 ± 85	124	XOSGUH01
Felodipine	C <sub>18</sub> H <sub>19</sub> Cl <sub>2</sub> NO <sub>4</sub>	294 ± 40	$\bar{4}11$	DONTIJ
Dutasteride	C <sub>27</sub> H <sub>30</sub> F <sub>6</sub> N <sub>2</sub> O <sub>2</sub>	220 ± 80	220	LATSIK
Amcinonide	C <sub>28</sub> H <sub>35</sub> FO <sub>7</sub>	130 ± 20	$1\bar{1}1$	VAYJOW
Probucol	C <sub>31</sub> H <sub>48</sub> O <sub>2</sub> S <sub>2</sub>	37 ± 10	020	HAXHET01
Efavirenz	C <sub>14</sub> H <sub>9</sub> ClF <sub>3</sub> NO <sub>2</sub>	33 ± 10	211	AJEYAQ02

As mentioned earlier diffraction spots fade as the cumulative dose increases due to the loss of crystallinity within the specimen. In some series, diffraction spots increase in intensity after the initial exposure and then sharply decrease towards zero (Figure 2) this is most probably due to movement/re-orientation of the crystal when irradiated.

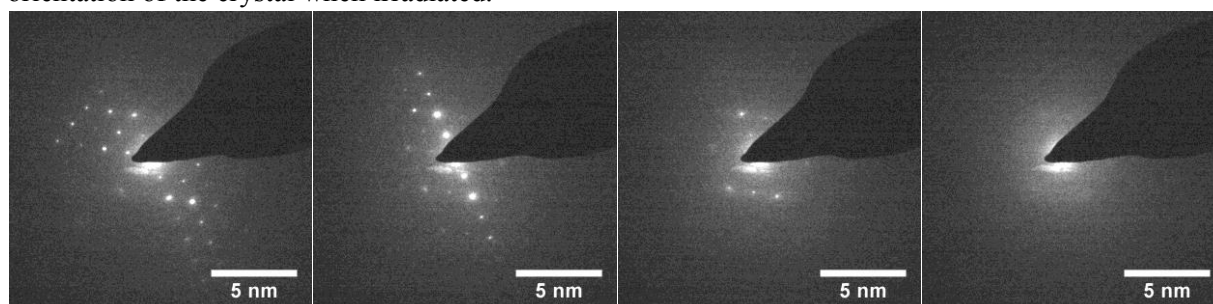


**Figure 2:** Diffraction pattern series of indapamide initially oriented on the [110] zone axis with electron flux of 3.59 electrons nm<sup>-2</sup> s<sup>-1</sup> at 45, 120, 170 and 250 seconds after initial exposure to the electron beam. The pattern changes to a systematic row after 120s before fading, consistent with a change in orientation of the crystal as well as a decrease in crystallinity.

Crystallinity decays with a number of different trends as shown by the normalised diffraction spot intensity versus cumulative electron fluence plots (Figure 3). The spot intensities increase and then decrease rapidly (Figure 3a), suggesting re-orientation of a crystal. Figure 3b shows the behaviour from the same sample but uses the ( $\bar{2}22$ ) spot rather than the ( $\bar{1}11$ ) spot. This plot shows a rapid decrease in intensity similar to the previous plot but without the movement/re-orientation. The values of characteristic dose are similar when estimated from each plot. The final trend is shown in both Figure 3c and 3d where there is a decrease in spot intensity followed by a stable plateau and then another decrease. An inverse power-law can be fitted to the final decrease at high fluence in each of the plots in Figure 3, similar to the fitting by Pan et al. who studied the electron beam induced damage of haemosiderin cores containing ferrihydrite [6].

When relating the structures of the pharmaceuticals (Table 1) to the average characteristic doses there are no obvious trends that describe the stability of molecular crystals in the electron beam. This includes characteristic dose and factors such as conjugated rings or halogens, which have been previously shown to increase the stability [4, 5]. Hence, there must be other parameters that contribute to the stability of the organic crystals. Possibilities include the lattice enthalpy (stability of crystal) or enthalpy of sublimation which relates to the intermolecular interactions within the crystal structure [8].

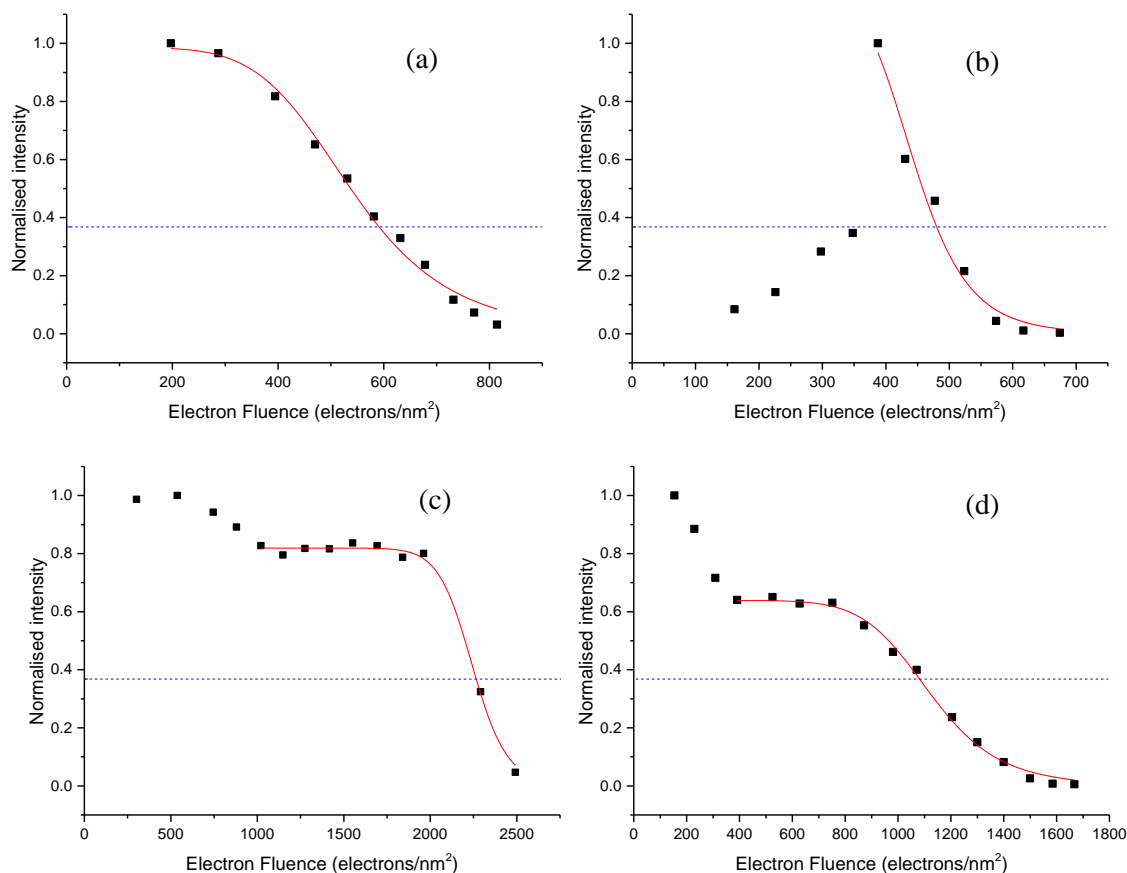


**Figure 3:** Normalized diffraction spot intensity versus cumulative electron fluence for specific diffraction spots in three different compounds. Red line is the fitting of the inverse power law and the blue line represents the value of  $1/e$  (a)  $(\bar{1}11)$  indapamide (b)  $(\bar{2}22)$  indapamide (c) tolinaftate, unknown diffraction spot (d)  $(\bar{1}11)$  griseofulvin.

#### 4. Conclusion

A low electron dose diffraction protocol for the characterization of pharmaceuticals has been successfully used giving indexed diffraction patterns and initial data on characteristic doses. The next challenge is to extend this protocol to drug formulations. Location of the API in the formulation matrix could also be identified by imaging, diffraction and even spectroscopy (EDX or EELS). Firstly, electron diffraction undertaken within the previously established dose limits can be used to determine the final crystal structure of the API. Secondly, API crystals which are nano-sized, and are therefore difficult to characterise by pXRD, could be characterised using this approach.

#### References

- [1] Eddleston M D, Bithell E G and Jones W 2010 *J. Pharma. Sci.* **99** 4072-4083
- [2] Egerton R F 2013 *Ultramicroscopy* **127**, 100-108
- [3] Egerton R F, Li P and Malac M 2004 *Micron* **35** 399-409
- [4] Li P and Egerton R F 2004 *Ultramicroscopy* **101** 161-172
- [5] Clark W R K, Chapman J N, Macleod A M and Ferrier R P 1980 *Ultramicroscopy* **5** 195-208
- [6] Pan Y H, Vaughan G, Brydson R, Bleloch A, Gass M, Sader K and Brown A 2010 *Ultramicroscopy* **110** 1020-1032
- [7] Allen F H 2002 *Acta Cryst* **B58** 380-388
- [8] Ouvrard C and Mitchell J B O 2003 *Acta Cryst* **B59** 676-685